Appl. Phys. B 66, 531–538 (1998)

Applied Physics B
Lasers
and Optics

Compact laser difference-frequency spectrometer for multicomponent trace gas detection

K.P. Petrov, R.F. Curl, F.K. Tittel

Rice Quantum Institute, Rice University, 6100 Main, Houston, TX 77005, USA
(Fax: +1-713/524-5237, E-mail: fkt@rice.edu)

Received: 14 August 1997/Revised version: 3 November 1997

Abstract. Design, performance characteristics, and application of a room temperature mid-infrared laser spectrometer are reported. This compact instrument is based on difference-frequency mixing of a widely tunable external-cavity diode laser and a diode-pumped monolithic Nd:YAG ring laser in periodically poled lithium niobate (PPLN). The difference-frequency tuning range of 3.98 μm to 4.62 μm was sufficient for detection of several atmospheric trace gases including carbon monoxide (CO), nitrous oxide (N_2O), carbon dioxide (CO_2), and sulfur dioxide (SO_2). Real-time detection of CO, N_2O, and CO_2 was performed in open air over a path length of 5 to 18 m. The feasibility of DFG spectroscopic measurement of the $^{13}C/^{12}C$ and $^{18}O/^{17}O/^{16}O$ isotopic ratios in atmospheric carbon dioxide was also investigated. We report what to our knowledge is the first simultaneous spectroscopic measurement of all three isotopes of oxygen in ambient CO_2.

PACS: 07:65; 33.00; 42.60; 42.65; 42.80

Application of laser difference-frequency generation (DFG) [1] to high-resolution spectroscopy of methane was first reported by Pine [2]. His experiment demonstrated not only the viability of a new method for generation of tunable mid-infrared light, but also its potential benefits to applications such as trace gas detection, chemical analysis, and industrial process monitoring. However, the use of Ar^+ and dye lasers as DFG pump sources in the field did not appear feasible because of their large size, fragility, and high power consumption.

Simon et al. [3] first obtained a tunable 4.7-μm difference-frequency output by mixing room-temperature diode lasers at 690 nm and 808 nm. Low output power (3 nW) in their experiment was not sufficient for use in high-resolution spectroscopy, but it demonstrated that diode lasers were suitable DFG pump sources. In a later experiment, Simon et al. [4] increased the difference-frequency output power to the microwatt level with the use of cavity-enhanced signal wave, at which point both high-resolution spectroscopy and sensitive trace gas detection appeared feasible. Subsequent tests by Petrov et al. [5] proved the feasibility of fast measurement of methane in ambient air to better than 12 ppb (parts in 10^9, by mole fraction). From this work it became clear that diode-pumped DFG gas sensors must meet two requirements in order to become an attractive choice for use in field applications. First, each sensor must be versatile enough to detect multiple gas species without interference from water vapor, either in-situ or over a long open path in air. This mandates a substantial tuning range, typically several hundred wavenumbers (Fig. 1), combined with an output power in excess of 10 μW cw. Second, the sensors must have a rugged optical construction in a small package, combined with low power consumption for portability.

Goldberg et al. [6] used high-efficiency and wideband quasi-phase-matching properties of bulk periodically poled lithium niobate (PPLN) for 3.3–4.1 μm tunable cw DFG with up to 0.5 mW output power, demonstrating coverage of the major portion of the wavelength region in Fig. 1. Balakrishnan et al. [7] reported the use of two high-power tunable diode lasers as pump sources in a PPLN-based

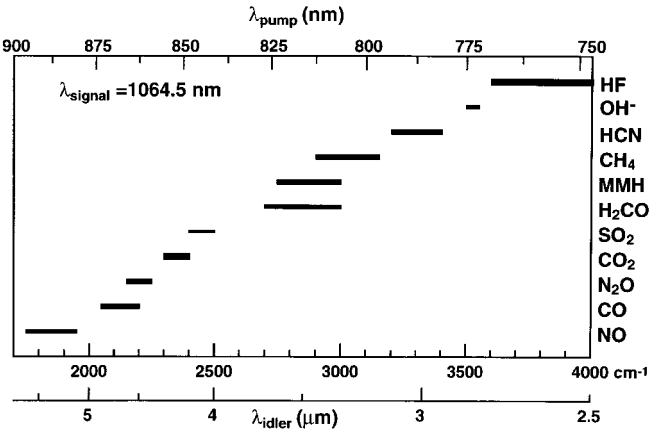

Fig. 1. Mid-infrared wavelength coverage by difference-frequency mixing of a tunable diode laser and a 1064.5 nm Nd:YAG laser. Goldberg et al. [6] demonstrated coverage of the 3.0–5.5 μm range by DFG in bulk periodically poled $LiNbO_3$. MMH is monomethyl-hydrazine, $N_2H_3CH_3$

difference-frequency spectrometer with up to 31 μW output power in the 3.34 to 4.35 μm region. At the same time, significant advances were made in the development of grating-tuned external-cavity diode lasers (ECDLs) [8, 9].

Reported herein are the design, performance characteristics, and application of an all-solid-state compact mid-infrared DFG laser spectrometer pumped by a widely tunable (842–865 nm) ECDL and a diode-pumped Nd:YAG laser at 1064.5 nm. The instrument employed a bulk PPLN crystal with eight domain grating periods from 22.4 to 23.1 μm. The tuning range of the spectrometer was from 3.98 μm to 4.62 μm, limited by the tuning range of the ECDL. The tuning range was sufficient for the detection of four atmospheric trace gases: CO, N_2O, CO_2, and SO_2. Real-time measurements of CO, N_2O, CO_2, and the $^{13}C/^{12}C$ isotopic ratio in CO_2 were performed in open air. We also report the first spectroscopic simultaneous measurement of all three isotopes of oxygen in atmospheric CO_2. All of the above measurements were accomplished with a single compact DFG source used in two different sampling configurations.

1 Instrument description

The spectrometer described herein consists of a laser difference-frequency source, an optical path through a gas sample, and a detector. Figure 2 shows a scaled diagram of the difference-frequency source. It is assembled on a 30 cm × 61 cm optical breadboard and employs two compact commercial lasers as pump and signal sources. The signal laser is a 700 mW diode-pumped monolithic Nd:YAG ring laser at 1064.5 nm (Lightwave Electronics, Inc., Model 126). The pump laser is a 16 mW tunable external-cavity diode laser (SDL, Inc., Model 8610). Tuning of the output wavelength from 842 nm to 865 nm was performed by rotation of its external diffraction grating. Continuous linear frequency scans of up to 80 GHz were performed by fine adjustment of the grating angle with a piezoelectric actuator, driven by a 50 Hz triangular wave. We found that after back-reflections into the ECDL had been eliminated by proper optical alignment, the remaining backscattering was insufficient to perturb single-frequency operation of the ECDL. The laser was therefore operated without optical isolation.

For difference-frequency mixing of the pump and signal lasers we used a 19-mm-long, 0.5-mm-thick PPLN crystal (Crystal Technology, Inc.) with domain grating periods from 22.4 μm to 23.1 μm in 0.1-μm steps. The eight domain gratings were arranged in 1.3-mm-wide strips spaced by 0.1 mm. Typical quasi-phase-matched difference-frequency (idler) power at the output of the PPLN crystal was 0.5 μW, with 11 mW incident pump power and 650 mW signal power. This amount of idler power is not sufficient for shot-noise-

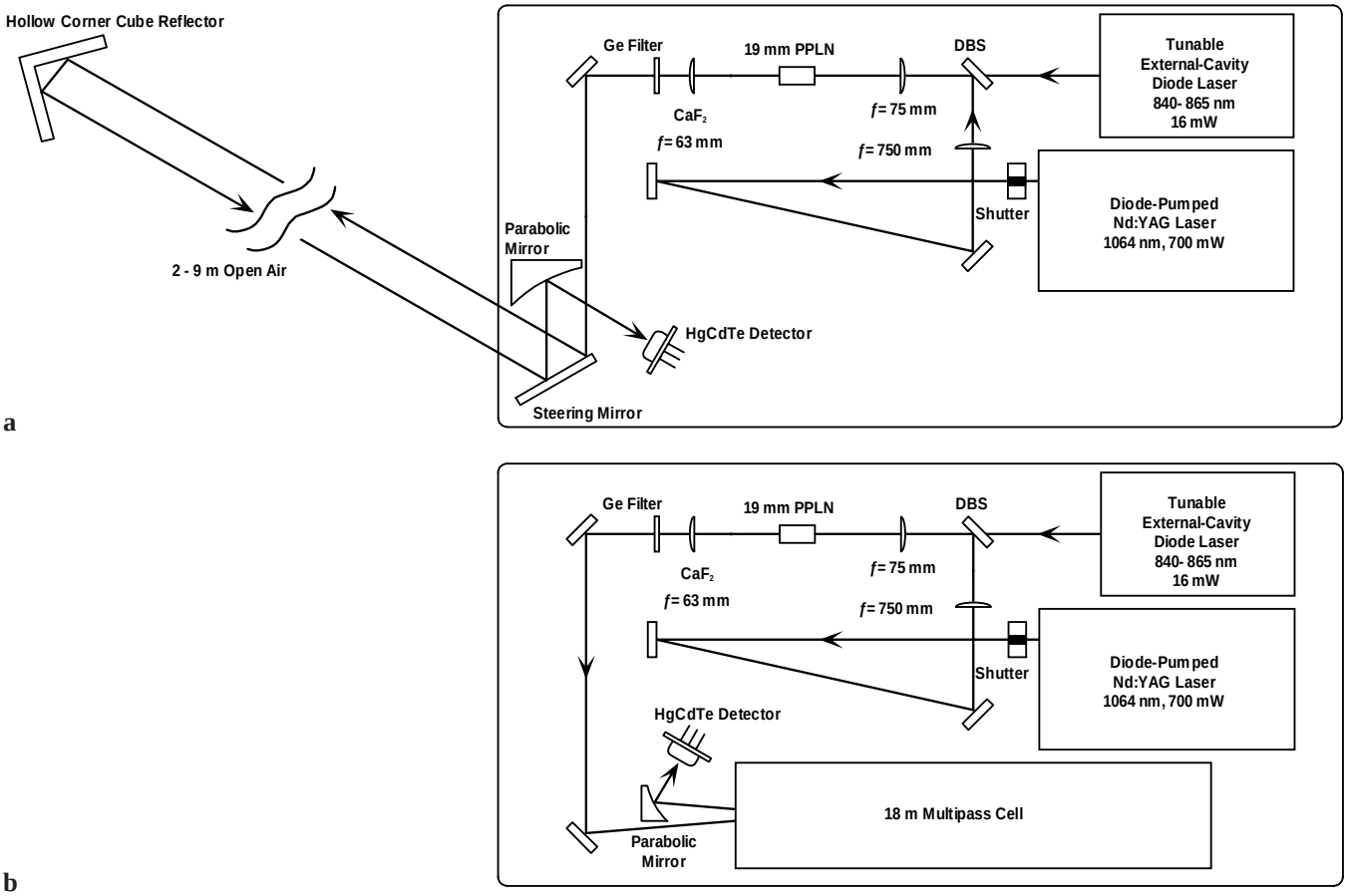

Fig. 2a,b. Scaled diagram of the compact (30 cm × 61 cm) diode-pumped difference-frequency spectrometer for multicomponent trace gas detection. Two air sampling configurations were used. Detection of CO, N_2O, and CO_2 was performed in open air (**a**) with the use of a single corner cube reflector. Detection of SO_2 and the $^{16}O/^{17}O/^{18}O$ isotopic ratio measurements in CO_2 were performed in a 18.3-m multipass cell (**b**) at reduced pressure

limited absorption measurements which become possible with the use of the lowest-noise InAs or HgCdTe infrared detectors and $> 10\,\mu$W idler power. An increase in the optical pump power from 11 mW to 500 mW using for instance a tunable discrete master oscillator power amplifier (MOPA), now commercially available, would provide an idler output power in excess of 20 μW. Antireflection coating of the input and output faces of the PPLN crystal would improve this number by factor of ~ 2.

The idler beam transmitted through a gas sample was measured with a Peltier-cooled photoconductive HgCdTe detector. The size of the detector element was 1 mm × 1 mm. Based on the calibrated detector response and the dark-noise measurements in the 0–25 kHz bandwidth, the noise-equivalent power of the detector was calculated to be 22 pW Hz$^{-1/2}$ at 4.6 μm. Low-drift biasing and dc coupling of the detector allowed the direct measurement of idler power necessary to determine percent optical absorption. The idler beam at the detector is blocked by a small mechanical shutter for 10 s every 3 min for the measurement of the dark offset voltage. The shutter is controlled by a laptop computer. The computer is equipped with a miniature 12-bit data acquisition card (National Instruments, Inc., Model DAQCard-1200) which is used to digitize the signal from the detector. Data acquisition is triggered by the function generator that performes linear frequency scans of the ECDL.

Two different configurations were used for the optical path through the gas sample. In the open path configuration (Fig. 2a), a collimated DFG beam was returned to the source by a hollow corner cube retroreflector (PLX, Inc.) with a circular aperture of 6.3 cm. The corner cube was placed at a distance of 2 to 9 m from the receiving mirror. Adjustment of the mirror tilt was used to point the DFG beam at the center of the corner cube for optimization of optical throughput, typically 80%. This arrangement allowed path-integrated measurements of trace gas concentration in open air.

Another sampling configuration (Fig. 2b) employed a compact multipass absorption cell with an effective path length of 18.3 m (New Focus, Inc., Model 5611). The cell was connected to a pump and used for trace gas measurements in air at reduced pressure. Both sampling configurations provided a small free space after the turning mirror (Fig. 2), suffficient to house a 10-cm-long reference absorption cell. The cell was filled with a low-pressure reference gas, usually nitrous oxide (N_2O), and could be moved in and out of the beam by a mechanical lever. Such an arrangement allowed the acquisition of absorption spectra of a sample gas overlapped with a Doppler-limited spectrum of a reference gas for wavelength calibration.

2 Detection of atmospheric trace gases

The spectroscopic information collected consisted of the detector voltage, $V(x)$, as a function of the frequency sweep signal to the diode laser controller, x, and the dark offset voltage V_{dark}. A time trace of detector voltage $V(x)$ averaged over 100 to 1000 sweeps, with V_{dark} subtracted, constituted a spectroscopic measurement. Depending on the number of averages, the result could be updated every 2 to 20 s. For short scans, the diode frequency, and thus the idler frequency, can be considered to be a linear function of x, $\nu = A + Bx$. The frequency sweep performed by a triangular waveform is nearly a linear function of time. Thus acquiring the detector voltage as a function of time is equivalent to acquiring it as a function of idler frequency ν.

The DFG output power showed weak nonlinear dependence on the sweep signal x. The etalon effect in the thin output window of the ECDL package was the primary cause of this nonlinearity. In the analysis described below it was modeled by a weak third-order polynomial $B_3(x)$. Transmission spectra were obtained by nonlinear least-squares fitting $\ln(V(x))$ to a superposition of the polynomial baseline and Voigt profiles [10] using the Levenberg–Marquardt method,

$$\ln\left(V\left(x\right)\right) = B_3\left(x\right) - \sum_i A_i \,\text{Voigt}\left(x - x_i,\, \gamma_i,\, \Delta\nu_i\right) \ .$$

Here A_i is the peak amplitude, x_i is the peak position, γ_i is the pressure-broadened halfwidth at half maximum of the peak, and $\Delta\nu_i$ is the Doppler halfwidth at $1/e$ of the peak. The number of peaks to be fitted, as well as peak position prior to fitting, were determined in each case from the HITRAN database [11], based on the knowledge of the calibrated DFG center wavelength. The fitted baseline was then subtracted from $\ln(V(x))$ to render the transmission trace $T(x)$.

$$T\left(x\right) = \exp\left(-\sum_i A_i \,\text{Voigt}\left(x - x_i,\, \gamma_i,\, \Delta\nu_i\right)\right) \ .$$

Direct absorption spectroscopy was chosen in this application because it offers adequate precision combined with the ease of signal processing and calibration. Alternatively, wavelength-modulation spectroscopy [12] can be used, provided the modulation frequency falls within the gain bandwidth of the detector/preamplifier. This method is attractive because of efficient reduction of noise bandwidth. However, it requires more sophisticated signal processing and calibration techniques.

The broad continuous tuning range (816–865 nm) available with some commercial ECDLs, when used in the difference-frequency setup, makes it possible to cover idler wavelengths from 3.50 μm to 4.62 μm. This wavelength range contains strong fundamental rovibrational absorption bands of several important trace air contaminants, including carbon monoxide (CO), nitrous oxide (N_2O), carbon dioxide (CO_2), formaldehyde (H_2CO), monomethyl-hydrazine ($N_2H_3CH_3$), and methane (CH_4). Detection and measurement of these and other species in air should therefore be possible with the use of a single DFG source such as the one described above.

Figure 3 shows an example of the high-resolution spectrum of nitrous oxide (N_2O) near 2169 cm^{-1}, acquired for the purpose of wavelength calibration. The fitted baseline was subtracted from the trace as described above. The frequency axis was linearized using the N_2O peak assignments of Maki and Wells [13]. The linearized axis contains 750 points with nearly uniform spacing of 36 MHz. The inset in Fig. 3 shows a close-up of the L-type doubled P28 transition of N_2O near 2169.33 cm^{-1}. The doublet is clearly resolved, suggesting that the worst-case linewidth of the DFG source is less than 150 MHz (0.005 cm^{-1}). Based on analysis of the magnitude of absorption peaks in Fig. 3 using the HITRAN database [11], we conclude that there is no appreciable

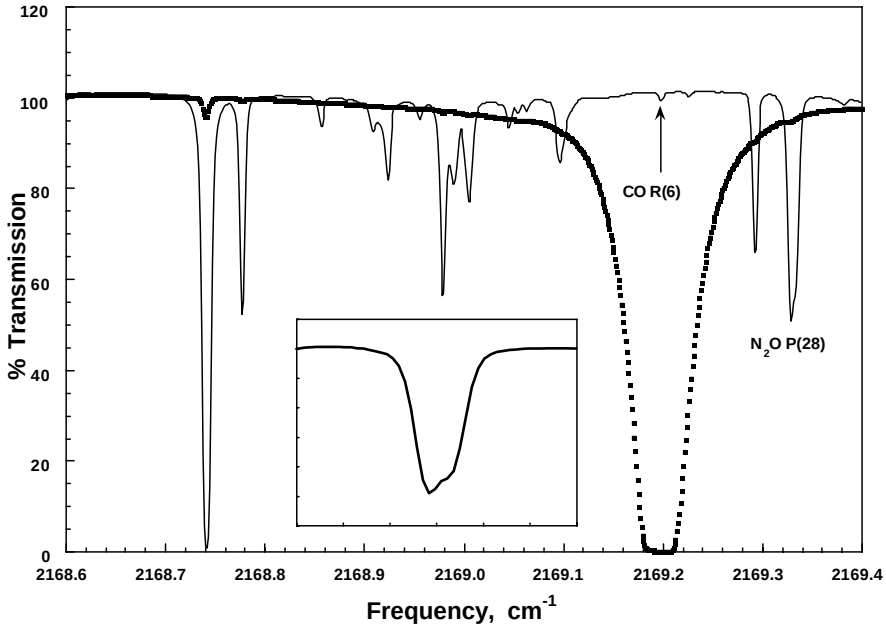

Fig. 3. High-resolution spectrum of N_2O in a 10-cm reference cell at 260 Pa. The *dotted line* shows a magnified section of the trace near 2169.33 cm^{-1}, featuring an L-type doubled P28 transition of N_2O. The transition is clearly resolved by the instrument, implying the worst-case DFG linewidth of < 150 MHz. The N_2O sample used in this measurement carried a small amount of CO impurity, and the residual absorption by R(6) of CO is observed near 2169.2 cm^{-1}

loss of signal due to convolution of the instrument lineshape and the absorption profile. We estimate therefore that the actual linewidth of the DFG source was less than 30 MHz, approximately 100 times smaller than the typical atmospheric pressure-broadened linewidth of most trace gases.

Figure 4 shows a spectrum of CO near 2169 cm^{-1} in ambient air. The spectrum was acquired using the open path configuration (see Fig. 2a) with 18-m path length. The full-scale idler power detected in this experiment was 0.41 μW. The signal was acquired for 2 s in a 0–25 kHz bandwidth, and represents a 100 sweep average. The fitted magnitude of the peak in an absorbance trace $a(\nu) = -\ln T(\nu)$ is $4.75(5) \times 10^{-2}$. The number in parentheses represents the uncertainty in the last significant digit. Based on the magnitude of peak absorbance, the molecular line strength of 4.51×10^{-19} cm [13], and the atmospheric-pressure-broadened halfwidth of 0.061 cm^{-1} [11], we compute a carbon monoxide concentration of 436 ± 5 ppb. We found earlier that this level of ambient CO, although higher than the US standard of 150 ppb [14], is typical for urban environment [15].

Figure 5 shows a spectrum of N_2O and $^{13}CO_2$ at 2236 cm^{-1} in ambient air. Signal acquisition conditions are the same as in Fig. 4. Significant absorption by ambient N_2O (having the typical abundance of 320 ppb [15]) is observed here with a signal-to-rms-noise ratio of 150, demonstrating the feasibility of a real-time measurement of ambient N_2O down to the 2-ppb level. Moreover, appreciable absorption by $^{13}CO_2$ suggests the feasibility of measurement of CO_2 using the isotopically shifted $00(0)1 - 00(0)0$ band, instead of the fun-

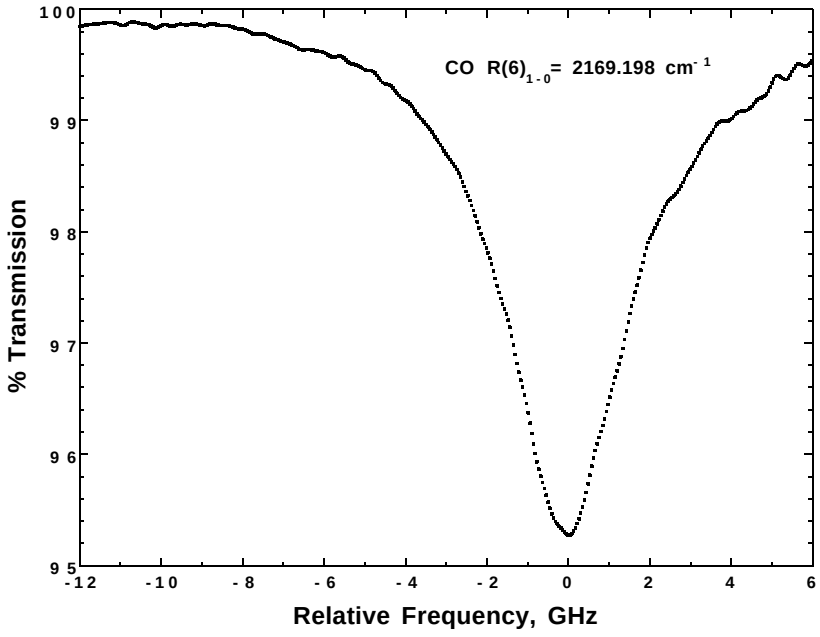

Fig. 4. Spectrum of the R(6) transition of CO in ambient air. The spectrum was acquired over 2 s using 18-m open path (see Fig. 2b), and is a 100 sweep average. The fitted magnitude of absorbance is $(4.75 \pm 0.05) \times 10^{-2}$, equivalent to 436 ± 5 ppb CO based on line strengths from Maki and Wells [13]

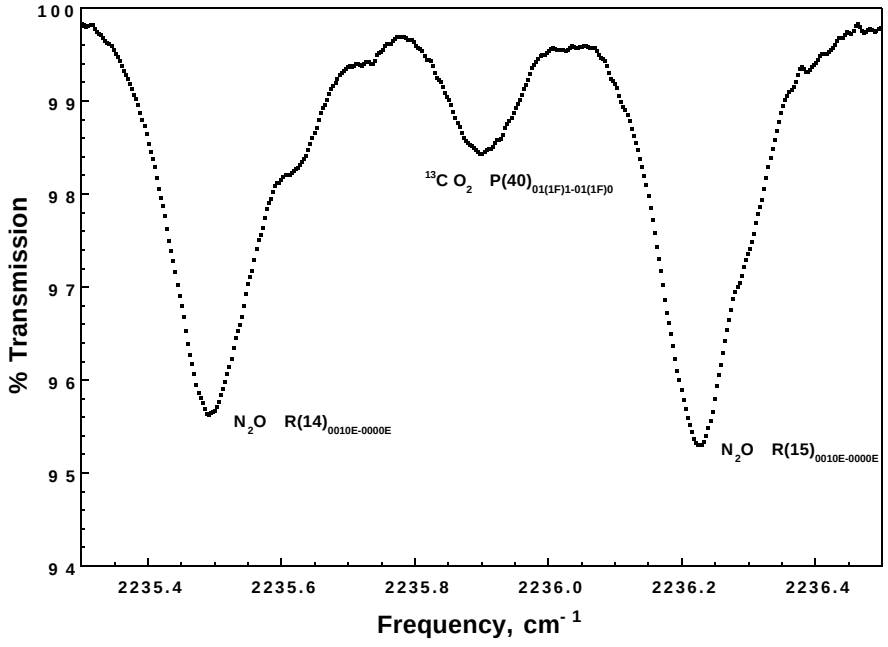

Fig. 5. Spectrum of ambient air near 2236 cm^{-1} showing absorption by N_2O and $^{13}CO_2$. The signal-to-noise ratio of 150 indicates the feasibility of measurement of ambient N_2O with a precision of bester than 2 ppb in 2 s

damental band. Atmospheric absorption in the fundamental $00(0)1-00(0)0$ band of carbon dioxide is very high because of its relatively high abundance and large transition dipole moment, restricting optical absorption measurements to path lengths shorter than 1 m. At lower frequencies, however, absorption strength of the fundamental $P_{00(0)1-00(0)0}$ branch of CO_2 decreases significantly, becoming comparable to that of the isotopically shifted $R_{00(0)1-00(0)0}$ branch of $^{13}CO_2$. It is then possible to detect both isotopes simultaneously over longer path lengths in air. Figure 6 shows a transmission spectrum of ambient CO_2 at 2296 cm^{-1}. Signal acquisition conditions are the same here as in Fig. 4, except the path length in open air was 5.5 m. The thin solid trace is a fit to a sum of six Voigt profiles with overall rms error of 1.9×10^{-3} absorbance units. The frequency axis was linearized based on the assignments of Guelachvili and Rao [16]. Fitted peak areas in the corresponding absorbance trace scale as

$$\begin{array}{c}\text{P45} : \text{R16} : \text{P56} : \text{P44}\\ 0.1681(4) : 0.7429(4) : 1.0000(3) : 0.1942(4)\end{array}$$

The numbers in parentheses represent the uncertainties in the last significant digits. Using the peak areas for R16 and P56, for example, one can measure the $^{13}C/^{12}C$ isotopic ratio in ambient CO_2 relative to that in a standard sample. We estimate, given the precision of our data, that such a relative measurement will be accurate to 9×10^{-4}. The normal isotope lines are weak enough to compare with the ^{13}C lines

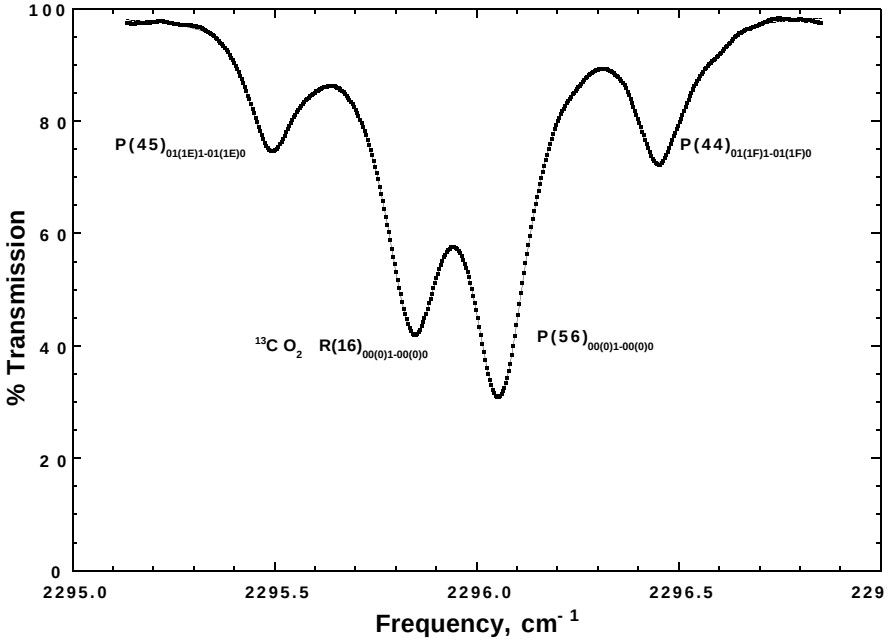

Fig. 6. Spectrum of CO_2 at 2296 cm^{-1} over 5.5-m open path in air. The signal was acquired for 2 s in a 25-kHz bandwidth and is a 100 sweep average *(dotted line)*. A *thin solid line* is a least-squares fit to a sum of six Voigt profiles. Fitted linear baseline $B_1(x)$ was subtracted from both traces

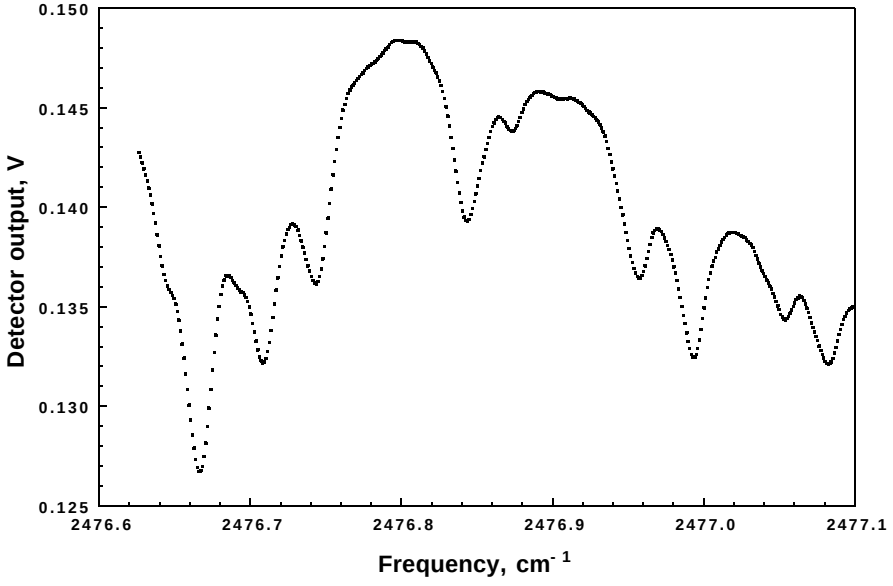

Fig. 7. High-resolution spectrum of SO_2 near 2477 cm^{-1}. The gas was kept in a 10-cm reference cell at 6 kPa. The trace shown is the detector output averaged over 1000 sweeps with dark voltage subtracted. Data were not fitted to remove the baseline

because their lower state is of relatively high energy making their populations small. This means that their absorption cross sections are sensitive to temperature and some care must be taken to make sure that the standard sample and the unknown are at the same temperature. This will be discussed further below.

Figure 7 shows a high-resolution spectrum of SO_2 in a 10-cm reference cell at 6 kPa. The spectrum was acquired over 20 s in a 0–25 kHz bandwidth and is a 1000 sweep average. The signal shown is the detector output $V(\nu)$ with dark voltage subtracted. The baseline contains broad interference fringes caused by the cell windows. The observed transitions belong to the combination band of SO_2 near 2477 cm^{-1}, and there is a considerable overlap between adjacent strong transitions even at low pressure. Baseline absorption in this case can be obtained (other than by removal of the sample) by tuning the DFG source outside the absorption band. However, the fine-tuning range of the pump laser was limited by the maximum excursion of the PZT-controlled feedback grating to less than 80 GHz which is insufficient for tuning outside the absorption band.

3 Measurement of oxygen isotopes in atmospheric CO_2

The trace gas detection capabilities of DFG can be extended for the measurement of isotopic ratios. Such a measurement, of the $^{13}C/^{12}C$ ratio in natural methane, using mid-infrared DFG was first performed by Waltman et al. [17]. Their measurement was based on comparison of optical absorption at the peak of two rovibrational transitions of significantly different strength. Here we compare frequency-integrated absorption from peaks of comparable strength, thereby improving measurement precision and reducing the effect of nonlinearity in the response of the infrared detector/preamplifier system. Our sample target species was carbon dioxide (CO_2), and the isotopic ratio of interest was $^{18}O/^{17}O/^{16}O$. Our interest was motivated primarily by the fact that ^{17}OCO can not be measured using mass spectrometry because the much more abundant isotopomer $O^{13}CO$ has the same molecular weight. Spectroscopic measurement of the $^{17}O/^{16}O$ ratio in atmospheric CO_2 also appeared difficult because of the requirement for high dynamic range in the measurement of the sum of optical absorption from both isotopes. We found, however, that the rotational band structure of carbon dioxide near 4.26 μm allows for simultaneous measurement of all three isotopes of oxygen while meeting the requirement of comparable absorption strength.

Figure 8 shows a transmission spectrum of room air at 3.6 kPa in an 18-m multipass cell (Fig. 2b). Prior to the measurement, a transmission spectrum of an empty cell was acquired to account for infrared absorption in surrounding air. Atmospheric transmission near 2349 cm^{-1} is very low due to partial overlap of pressure-broadened strong absorption lines P(1) and R(0) of the fundamental isotope of CO_2. However, the overlap disappears at reduced pressure, creating an infrared-transparent spectral window suitable for the measurement of the $^{18}O/^{17}O/^{16}O$ isotopic ratio in atmospheric CO_2. The thin solid trace in Fig. 8 is a least-squares fit to a sum of three Voigt peaks, with root-mean-squared deviation of 0.0014 absorbance units. The frequency axis was constructed by matching the fitted peak centers to their assignments by Guelachvili and Rao [16]. This procedure can be used to linearize the frequency axis, which is particularly useful with long wavelength scans allowing correct calculation of the peak area. The fitted peak areas scale as 4.958(6):1.163(6):1.300(6), versus 5.31:1.22:1.30 computed at 296 K using the HITRAN database [11]. We estimate, given the precision of the peak area measurement, that the $^{18}O/^{17}O/^{16}O$ isotopic ratio in CO_2 can be determined relative to that of a standard sample with a precision of better than 5×10^{-3}, provided adequate precision is maintained in the control of gas temperature. The lower state of the R37 transition is 1885.5 cm^{-1} [11], and we estimate that the temperature of the gas must be kept the same in the comparison of the unknown sample to the reference sample to within about 0.2 °C. The uncertainty in determination of peak area (last significant digit given in parentheses), is limited by optical interference fringes from scattering in the multipass cell. We did not attempt to reduce the effect of interference by apply-

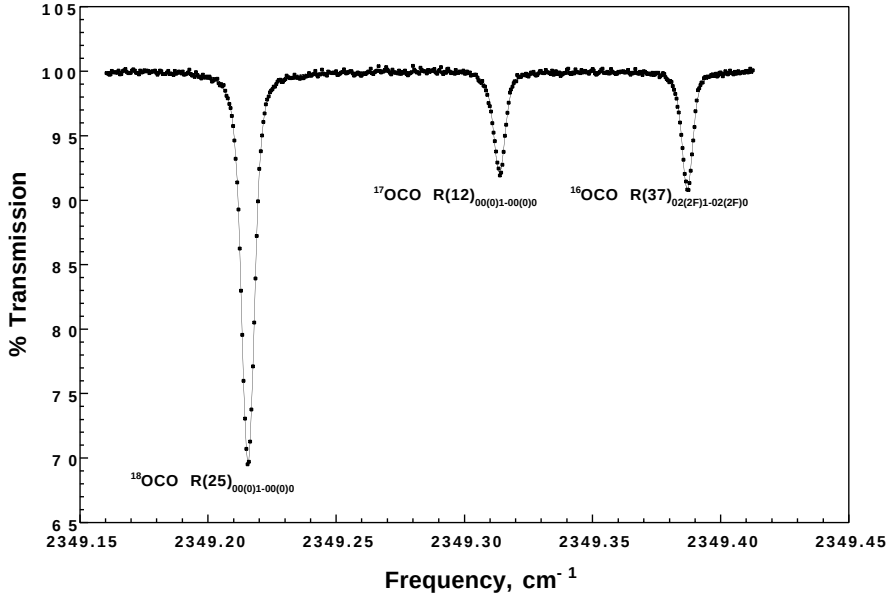

Fig. 8. Mid-infrared spectrum of the oxygen isotopes of CO_2 in room air at 3.6 kPa inside an 18.3-m multipass cell (see Fig. 2a). The spectrum was acquired in 2 s and is a 100 sweep average

ing vibration to the cell, as reported earlier [18], although it has been shown to reduce the interference down to or below the detector noise level. With the use of interference cancellation down to detector noise level the measurement precision should improve to 10^{-4}; however, the comparisons must then be made with unknown and reference samples at the same temperature to within 0.003 °C. At this temperature control level, heating through the vibration of the cell and heating by the infrared absorption may be significant.

4 Summary

This work describes the design and performance characteristics of a compact room-temperature DFG spectrometer capable of real-time measurement of four atmospheric trace gases: CO, N_2O, CO_2, and SO_2. The instrument employs quasi-phase-matched PPLN crystal with multiple grating periods (22.4 μm to 23.1 μm with 0.1 μm steps), pumped by two single-frequency solid-state lasers, and a Peltier-cooled HgCdTe infrared detector. The pump laser is an external-cavity diode laser with 16 mW output power tunable from 842 to 865 nm. The signal laser is a diode-pumped monolithic ring Nd:YAG laser at 1064.5 nm. The difference-frequency output of 0.5 μW was tunable from 3.98 to 4.62 μm (10.4 THz) with less than 30 MHz linewidth. The tuning range was limited by the single-frequency tuning range of the pump laser.

The DFG spectrometer was used for real-time spectroscopic measurement of CO, N_2O, and CO_2 in open air. Spectral scans of 80 GHz at the rate of 50 Hz were performed by rotation of a PZT-driven feedback grating of the pump ECDL. The precision of measurement of gas concentration in ambient air with a signal averaging time of 2 s was better than 5 ppb for CO, better than 2 ppb for N_2O, and better than 100 ppb for CO_2. We demonstrated the feasibility of relative measurement of the $^{13}C/^{12}C$ isotopic composition of CO_2 in open air to better than 9×10^{-4}. We also demonstrated, for the first time, simultaneous spectroscopic measurement of the $^{18}O/^{17}O/^{16}O$ isotopic ratios in atmospheric CO_2. The development of this technology for field measurement of oxygen isotope ratios requires much more work on calibration, temperature control, and measurement protocols.

A promising development of this technology would involve the use of quasi-phase-matched PPLN waveguides [19] in conjunction with fiber-coupled low-power diode lasers. Arbore et al. [20] reported DFG conversion efficiencies of up to 3% W^{-1} for adiabatically tapered, periodically segmented PPLN waveguides. With such high conversion efficiency per device one can obtain DFG output power approaching the 0.1-mW level with only 50 mW of pump and signal power, making shot-noise-limited absorption measurements possible. The use of fiber-coupled pump and signal lasers should allow construction of a compact, rugged, alignment-free optical train.

Acknowledgements. The authors are grateful to Dr. John Graf of the NASA Johnson Space Center and Dr. Edward Dlugokencky of NOAA Boulder for helpful discussions. The authors also thank Bruce Brinson of Rice University for valuable technical assistance. The work was supported in part by the NASA Johnson Space Center, the U.S. Department of Energy, the Texas Advanced Technology Program, the National Science Foundation and the Robert A. Welch Foundation.

References

1. G.D. Boyd, D.A. Kleinman: J. Appl. Phys. **8**, 3597 (1968)
2. A.S. Pine: J. Opt. Soc. Am. **66**, 97 (1976)
3. U. Simon, C.E. Miller, C.C. Bradley, R.G. Hulet, R.F. Curl, F.K. Tittel: Opt. Lett. **13**, 1062 (1993)
4. U. Simon, S. Waltman, I. Loa, L. Hollberg, F.K. Tittel: J. Opt. Soc. Am. B **2**, 1 (1995)
5. K.P. Petrov, S. Waltman, U. Simon, R.F. Curl, F.K. Tittel, E.J. Dlugokencky, L.W. Hollberg: Appl. Phys. B **61**, 553 (1995)
6. L. Goldberg, W.K. Burns, R.W. McElhanon: Opt. Lett. **20**, 1280 (1995)
7. A. Balakrishnan, S. Sanders, S. DeMars, J. Webjörn, D.W. Nam, R.J. Lang, D.G. Mehuys, R.G. Waarts, D.F. Welch: Opt. Lett. **21**, 952 (1996)
8. C.E. Wieman, L.W. Hollberg: Rev. Sci. Instrum. **62**, 1 (1991)
9. F.J. Duarte (Ed.): *Tunable Laser Applications* (Dekker, New York 1995) p. 83

10. J. Humlicek: J. Quant. Spectrosc. Radiat. Transfer **21**, 309 (1979)
11. L.S. Rothman, R.R. Gamache, A. Goldman, L.R. Brown, R.A. Toth, H.M. Pickett, R.L. Poynter, J.-M. Flaud, C. Camy-Peyret, A. Barbe, N. Husson, C.P. Rinsland, M.A.H. Smith: Appl. Opt. **26**, 4058 (1987)
12. F.S. Pavone, M. lnguscio: Appl. Phys. B **56**, 118 (1993)
13. A.G. Maki, J.S. Wells: *Wavenumber Calibration Tables From Heterodyne Frequency Measurements*, NIST Special Publication 821 (1991)
14. D.K. Killinger, J.H. Churnside, L.S. Rothman: In *Handbook of Optics*, Vol. I, *Fundamentals, Techniques, and Design*, 2nd edn., ed. by M. Bass, E.W. Van Stryland, D.R. Williams, W.L. Wolfe (McGraw-Hill, New York 1995) p. 5
15. K.P. Petrov, Y. Mine, T. Töpfer, R.F. Curl, F.K. Tittel: Society of Automotive Engineers (SAE) Technical Digest Series '97, paper no. 97ES-175 (July 16, 1997)
16. G. Guelachvili, K.N. Rao: *Handbook of Infrared Standards* (Academic Press, New York 1986)
17. S. Waltman, L.W. Hollberg, K.P. Petrov, F.K. Tittel, E.J. Dlugokencky, M.A. Arbore, M.M. Fejer: "Measurement of $^{13}CH_4/^{12}CH_4$ Ratios in Air Using Diode-Pumped 3.3 μm Difference-Frequency Generation in PPLN", Proceedings of the 1997 IEEE/LEOS Summer Topical Meeting, Montreal (11–15 August 1997)
18. K.P. Petrov, S. Waltman, E.J. Dlugokencky, M.A. Arbore, M.M. Fejer, F.K. Tittel, L.W. Hollberg: Appl. Phys. B **64**, 567 (1997)
19. M. Bortz: "Quasi-Phasematched Optical Frequency Conversion in Lithium Niobate Waveguides", Ph.D. dissertation, Edward L. Ginzton Laboratory, Stanford, CA 94305 (December 1994)
20. M.A. Arbore, M.H. Chou, M.M. Fejer: CLEO Technical Digest Series **9**, 120 (1996)